J Mater Sci (2007) 42:50–58
DOI 10.1007/s10853-006-1045-0

Microstructure and stresses in a keatite solid–solution glass–ceramic

Christian Roos · Otmar Becker · Friedrich Siebers

Received: 19 October 2005 / Accepted: 17 January 2006 / Published online: 11 November 2006

Abstract The microstructure of a translucent keatite solid–solution glass–ceramic (keatite s.s.) of the LAS-system (Li_2O–Al_2O_3–SiO_2) has been analyzed with SEM, AFM, XRF, XRD, and TEM. The glass–ceramic consists mainly of keatite s.s. with minor secondary phases such as zirconium titanate, gahnite and probably rutile. Furthermore the resistance to temperature differences (RTD) of this glass–ceramic was investigated. It is shown that, in spite of the relatively high coefficient of thermal expansion (CTE) of about 1×10^{-6} K^{-1}, an improved RTD can be achieved by special ceramization treatment. With this, compressive stresses in the first 100 μm to 150 μm are induced. These stresses can presumably be contributed to a difference in CTE between the surface-near zone and the bulk. Said CTE difference is caused by chemical gradients of CTE-relevant elements, such as Zn, K, and supposedly additional alkali elements such as Li. These stresses are useful to increase the strength and application range of glass–ceramics based on keatite s.s.

Abbreviations

LAS	Li_2O–Al_2O_3–SiO_2
HQ	High-quartz
CTE	Coefficient of Thermal Expansion
RTD	Resistance to Temperature Differences
s.s.	solid–solution
SEM	Scanning-Electron Microscopy
TEM	Transmission Electron Microscopy
EDX	Energy Dispersive X-ray Spectroscopy
XRF	X-ray Fluorescence Analysis
XRD	X-ray Diffraction
RS-XRD	Residual-Stress X-ray Diffraction

C. Roos (✉) · O. Becker · F. Siebers
Corporate Research and Technology Development,
SCHOTT AG, Hattenbergstraße 10, Mainz 55122, Germany
e-mail: christian.roos@schott.com

Introduction

During the past decades transparent glass–ceramics of the LAS-system (Li_2O–Al_2O_3–SiO_2), mainly consisting of high-quartz solid solution (hQ s.s.), have been established as a very suitable material when high resistance to temperature differences (RTD), e.g. for cooktop panels, is required. An outstanding advantage of these materials is their low coefficient of thermal expansion (CTE) of about 0.2×10^{-6} K^{-1} (measured from 20 °C to 700 °C). Because of this, in wide temperature ranges simply no harmful stresses due to temperature differences during heating are induced [1].

With further heat-treatment the metastable hQ s.s. transforms into keatite solid solution (keatite s.s.). Recently, glass–ceramics consisting mainly of keatite s.s. have gained more and more attention because of their adjustable translucent and opaque appearance and colourability. An advantage of keatite s.s.-based glass–ceramics is their lower content of residual glass phase and lower expansion anisotropy, which lead to higher fracture strength. The larger crystals (>300 nm) cause a translucent appearance, which is also desirable because of design variations. A disadvantage of keatite

s.s. glass–ceramics is their CTE of about $1 \times 10^{-6}\,K^{-1}$, which makes them more prone to failure due to thermal shock.

Surface-compressive stresses in brittle materials, such as glass–ceramics, can lead to an increase in fracture strength, whereas tensile stresses are in most cases fatal. Especially when subjected locally to thermal load, tensile-stresses in cold areas can be induced, which subsequently lead to crack initiation and failure. A possibility for introducing compressive stresses in LAS-glass–ceramics is the abortion of the hQ s.s. to keatite s.s. transformation at halfway: Because the transformation starts in the bulk, the CTE-difference (between hQ s.s. at the surface and keatite s.s. in the bulk) induces compressive stresses in the surface of the material [2]. Nevertheless, temperature-control in such a ceramization process is very difficult and the long-term stability of such a material is questionable [3].

In this paper the microstructure of a translucent keatite s.s. glass–ceramic (which is transformed to a stable assemblage in bulk and surface) is investigated. It is discussed how, in spite of the relatively high CTE, the RTD can be increased by inducing compressive stresses into the surface of the material *without* aborting the transformation.

Experimental and theoretical considerations

A glass with a constant composition was transformed into a keatite s.s. glass–ceramic with various defined heat-treatments, all at a maximum temperature (T_{max}) of 1100 °C. The glass contained 20.0 wt% Al_2O_3, 67.2 wt% SiO_2, 3.4 wt% Li_2O, 1.5 wt% ZnO, and 1.2 wt%MgO as crystal-relevant compounds; 2.6 wt% TiO_2 and 1.8 wt% ZrO_2 as nucleation agents and 1.5 wt% alkali- and earth-alkali compounds for better melting and building of the glassy matrix. The amount of 0.8 wt% fining agent was used. It was found that the RTD can be controlled between approx. 660 °C and 780 °C with different adjusted ceramization programs, but without changing T_{max} and time at T_{max}. In the following, the programs used for manufacturing and the samples thereof are named by P_XXX, where XXX stands for the average RTD of the program.

The microstructure of the above described glass–ceramic was investigated with a scanning electron microscope (SEM), type LEO Gemini 1550. The samples were etched for 45 s in a 1:1 mixture of 2 vol% hydrofluoric acid/10 vol% sulphuric acid to reveal the crystals, and coated with a 6 nm gold-layer to provide electron conductivity.

Transmission electron microscopy (TEM) coupled with energy dispersive x-ray spectroscopy (EDX) was used to determine the distribution of the secondary phases and to investigate the residual glassy phase. The analysis was carried out on a Philips CM12 equipped with an EDAX PV 9800 system. The samples were thinned to electron transparency in an ion-mill type Gatan 610. In previous analysis it was proven (by comparison of cooled and not cooled samples) that the microstructure of the glass–ceramic is not altered when subjected to the electron-beam. Similar results on the stability of keatite s.s. glass–ceramics have been obtained earlier [4].

Chemical composition and also chemical gradients were measured by x-ray fluorescence analysis (XRF) with a Philips PW2404 MagiXPro, the latter by careful polishing of the material in steps of 10 μm and using low-energy lines. A distribution coefficient was recorded for each element by calculating the ratio "$\text{Intensity}_{\text{element surface-near}}/\text{Intensity}_{\text{element bulk}}$". It was proven that no changes in the element distributions occurred from 400 μm depth on. Therefore, measurements at 400 μm were taken as reference point (constant bulk concentration).

X-ray diffraction (XRD) and residual-stress x-ray diffraction (RS-XRD) were done on a Philips MRD with $Cu_{K\alpha}$-radiation, and on a Siemens D5005 with $Cr_{K\alpha}$-radiation respectively. For powder diffraction a $K_{\alpha 1}$-monochromator was used.

The RTD was measured by locally heating crystallized plates with the dimension 250 mm × 250 mm × 4 mm until breakage. For detailed description of the RTD-testing method refer to the literature [5]. The breakage temperature was recorded and is referred to as "RTD"[1], as explained later. Young's modulus E and Poisson-ratio ν of the material where determined to be 86 GPa and 0.211, respectively, and no significant changes in these material properties where observed as long as T_{max} and time at T_{max} were kept constant.

Residual stresses were also measured with a Vickers indentation method. This method correlates the fracture toughness K_{Ic} with the residual stresses in the material. Surface stresses of compressive or tensile nature inhibit or promote the growth of cracks, which are induced e.g. by Vickers indentation. The length of the surface cracks can be used as a relative measure of the existing stresses. This method

[1] Because RTD stands for "resistance to temperature difference" it describes strictly speaking a strength [MPa]. Nevertheless according to Eq. (4) here the breakage-temperature [°C] is used as a measure of RTD.

is not suitable for absolute stress measurement, but it is highly useful for relative measurements. The indentations where done with a Zwick Z 2.5 testing machine with at least 30 indentations per sample, followed by crack-length measurements with a light microscope. The theory of Vickers indentation is extensively described elsewhere [6–8]. Because the use of Vickers indentation for stress-measurement is not well known, the theoretical considerations are briefly explained here:

Crack length c_i and indenter diagonal a of an indent are measured. The fracture toughness K_{Ic} is then described by

$$K_{Ic} = f_1 H\sqrt{a}\cdot\left(\frac{E}{H}\right)^{1/2}\left(\frac{a}{c_i}\right)^{3/2} \quad \text{with} \quad H = \frac{F}{2a^2} \tag{1}$$

where F is the indentation load. For half-penny cracks the geometry factor f_1 is 0.032 [9]. No variations in E or v where observed in all tested samples, therefore it was for the sake of clarity useful to consider the hardness H, which here corresponds to Vickers hardness, as constant. Then

$$K_{Ic} = \frac{1}{2} f_2 \left(\frac{E}{H}\right)^{1/2} \frac{F}{c_i^{3/2}} \tag{2}$$

is a direct measure for the fracture toughness, where $F/c_i^{3/2}$ is a proportional factor derived from load and induced crack length. The maximum stress is described as:

$$\sigma_{max} = \frac{1}{f_3}\frac{K_{Ic}}{\sqrt{c_i}} \tag{3}$$

with $f_3 = 1.99$ [9]. The fracture strength σ_{max} is qualitatively correlated with the maximum tangential fracture strength $\sigma_{tan(R)}$ when RTD is tested, which is described by

$$\begin{aligned} \Delta T &= T_b - T_a = \frac{1}{f_1}\cdot\frac{\sigma\cdot(1-v)}{\alpha\cdot E} \quad \text{resp.} \\ \sigma_{tan(R)} &= f_1\cdot\frac{\alpha\cdot E}{(1-v)}\cdot(T_{max}-T_R) \end{aligned} \tag{4}$$

where T_b is the temperature at the hotter position b and T_a is the temperature at the colder position a. If the temperature at the hottest region of the material is T_{max} and the temperature at the coldest region is T_R, $\sigma_{tan(R)}$ is the maximum tangential (and therefore fracture-relevant) stress that can occur. Based on Eqs. (3) and (4), the correlation between RTD and K_{Ic} is:

$$RTD \propto \frac{K_{Ic}}{\sqrt{c_i}}\frac{(1-v)}{\alpha\cdot E} \tag{5}$$

When examining a stressed material, special considerations have to be made: If the thickness d of the stressed layer is much greater than the induced crack length c_i ($d >> c_i$) the material within the crack length can be considered as uniformly strained [10, 11]. In case of $d \le c_i$, the K_{Ic} is described as

$$K_{Ic} = \frac{1}{2} f_2 \left(\frac{E}{H}\right)^{1/2} \frac{F}{c_i^{3/2}} + 2 f_4 \sigma_s \sqrt{d} + f_4 \sigma_b \sqrt{c_i} \tag{6}$$

with σ_s as the average residual stress of the layer. σ_b describes the stress in the bulk below the stressed layer. f_4 is a geometry factor, here determined as $f_4 = 1$. The fracture toughness therefore results from a combination of the bulk fracture toughness and additional layer stresses. Because of the third term, the correlation between F and $c_i^{3/2}$ deviates with higher load and deeper cracks from linear behaviour.

If the thickness of the compressive layer is much smaller than the induced crack length ($d << c_i$,), the surface crack length is different to the bulk crack length. Under these conditions special considerations are needed.

Results and discussion

Structure and chemistry of the glass–ceramic

When discussing the structure of the ceramized glass–ceramic, it should be noted that no significant differences in materials ceramized with different heat-treatments P_665, P_692, P_721, P_730, P_756, and P_777 (constant T_{max} and time at T_{max}) could be detected by means of XRD, SEM, and TEM. In the following the results for the material P_730 are shown.

The diffraction pattern of the material is shown in Fig. 1 and the phase composition was determined by Rietveld analysis to be mainly keatite s.s. ($LiAlSi_2O_6$, JCPDS 35-794) with less than 3 wt% zirconium titanate ($ZrTiO_4$, JCPDS 34-425) and less than 1 wt% gahnite ($ZnAl_2O_4$, JCPDS 5-669). The amount of residual glassy phase was less than 10 wt%. With powder-XRD no other phases could be detected.

The microstructure of the surface and of the bulk is shown in SEM-micrographs (Figs. 2 and 3). After the commonly known surface structure with a glassy zone and a thin layer of hQ s.s crystals, keatite s.s is the predominant phase. The crystals are between 500 nm

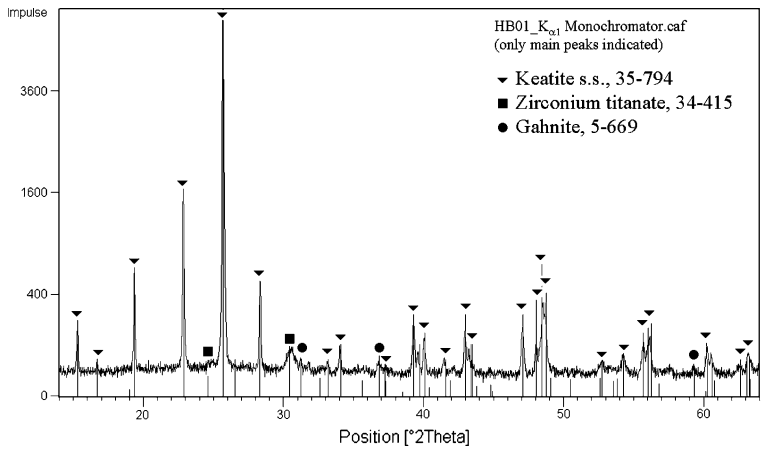

Fig. 1 Powder XRD of the investigated glass–ceramic

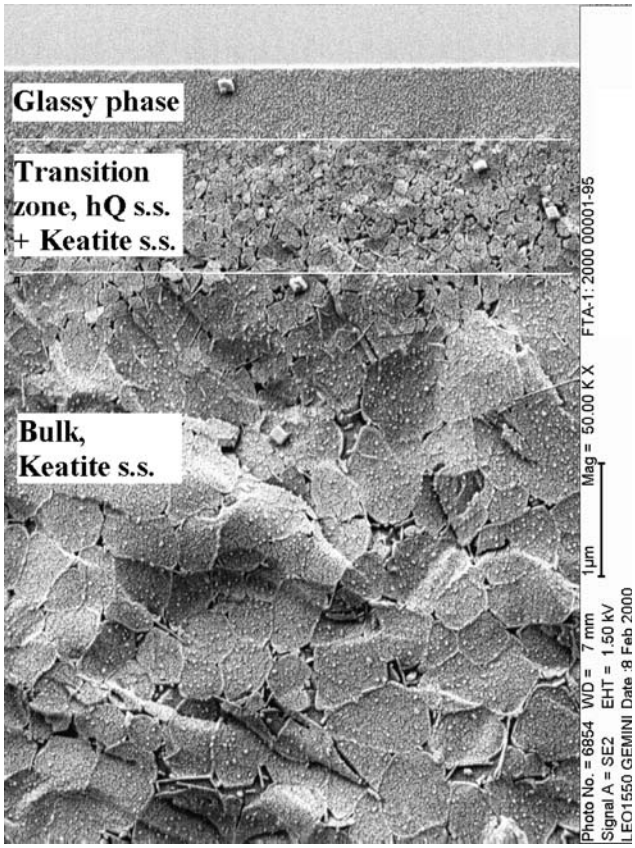

Fig. 2 SEM-micrograph of the etched glass–ceramic, surface cross-section

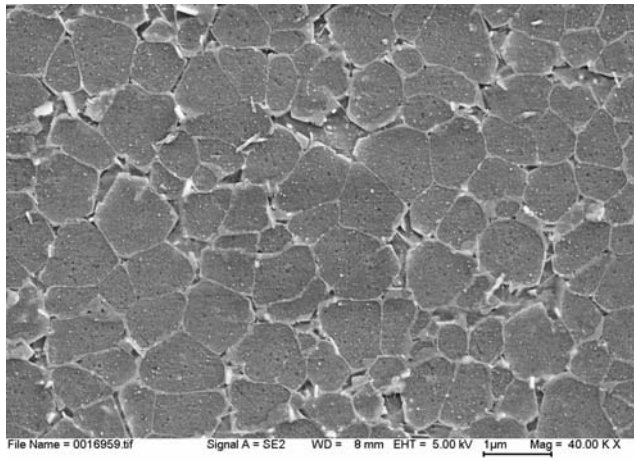

Fig. 3 SEM-micrograph of the etched glass–ceramic, bulk cross-section

and 800 nm in diameter and uniformly distributed. The microstructure is homogenous and the grain boundaries appear slightly brighter in the electron beam. This is due to a stronger phase contrast of the secondary phases, which are dominant at the grain boundaries and contain the heavier elements Zn, Ti, and Zr. These secondary phases are less sensitive to the wet-chemical etching, which is necessary to reveal the grain boundaries. Therefore, the grain boundaries are topographically higher, as can be seen from the corresponding AFM-image in Fig. 4.

The amount of glassy phase and the crystal size[2] were determined by a commercial computer-supported microstructure analysis (Image C) to be between 7–10 vol% and 600-1000 nm, respectively, as shown in Figs. 5 and 6. The values showed no significant variations from the surface up to a depth of 100 µm. They can be assumed to be constant over the complete thickness of the material based on the SEM-images of the bulk. The near-surface region was not considered here because of the mentioned layered structure.

As proven with TEM, the glassy phase remains in pockets and no continually 3-dimensional network is formed. It is possible, however, that the contact zone between two keatite s.s. crystals is distorted in the nm-range and shows no crystal-structure.

[2] The bars in the average grain-size diagram show the cross-sectional distribution, not the error of the analysis.

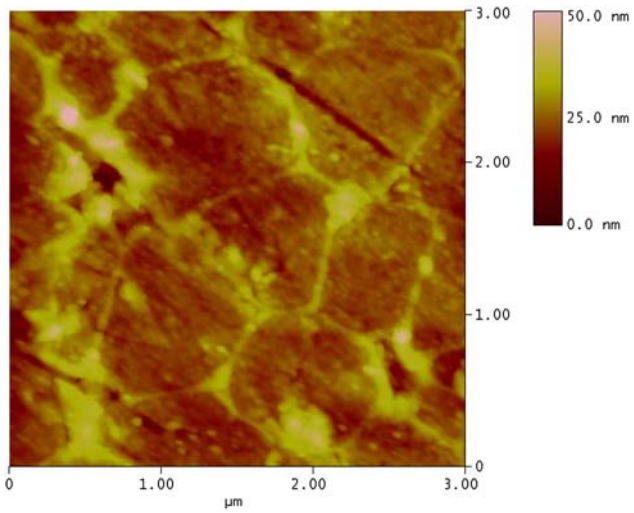

Fig. 4 AFM-Image, bulk cross-section of the etched glass–ceramic

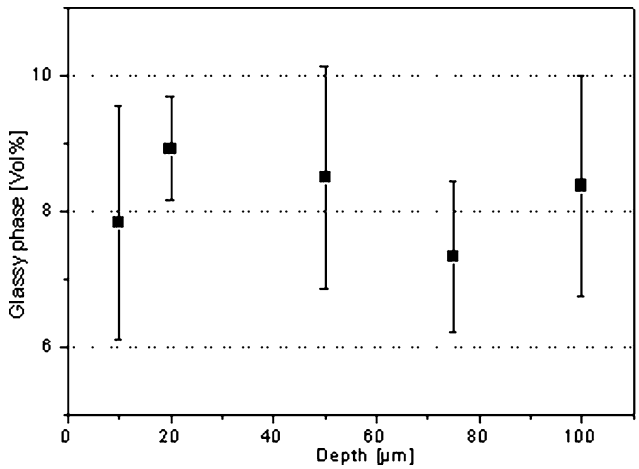

Fig. 5 Distribution of the amount of glassy phase over depth

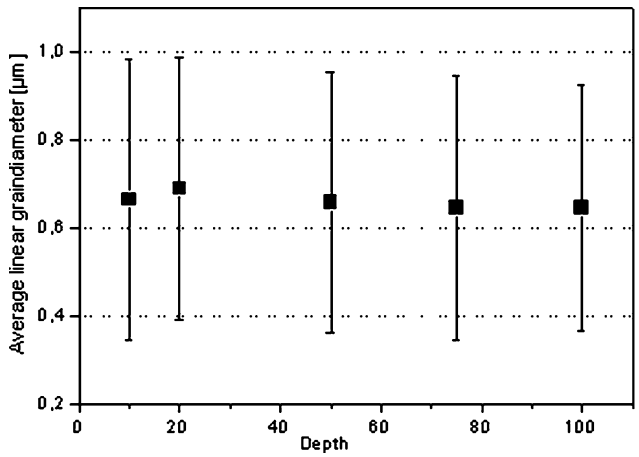

Fig. 6 Average grain diameter over depth

In Fig. 7 the secondary-phases, as identified with electron diffraction and EDX, are labelled with numbers 1–4. The keatite s.s. can be clearly seen in the centre of the image. Gahnite (no. 1) was found at grain boundaries. Zirconium titanate crystals (no. 2) were found at grain boundaries and inside the keatite s.s.. The glassy phase (no. 3) showed a high Si/Al-ratio and a significant amount of As and Ba. This confirms, as is to be expected, that As and Ba are incompatible with the keatite s.s. structure. The sum of fining agents and earth-alkali compounds in the green-glass composition is approximately 1,5 wt%. This amount leads with further crystallisation of keatite s.s. to an enrichment of up to 15 wt% in the residual glassy phase. In the TEM-image also small needles (no. 4) can be seen, which could not be identified with electron-diffraction. EDX-analysis of these needles showed a strong Ti-signal. These needles are therefore very likely to be TiO_2, and referring to the temperature history of the material with a $T_{max} > 1000$ °C presumably rutile. In XRD-scans no rutile could be detected, but the observed needles might be too small in size and therefore X-ray-amorphous (<15 nm) and/or below the detection limit (<1 wt%).

Besides the ceramization-processes at a constant T_{max}, additional heat treatments were carried out to investigate the transformation behaviour of the keatite s.s. crystals. Here, no significant visible changes in the microscopic structure of the glass–ceramic could be detected except a decrease of the amount of the

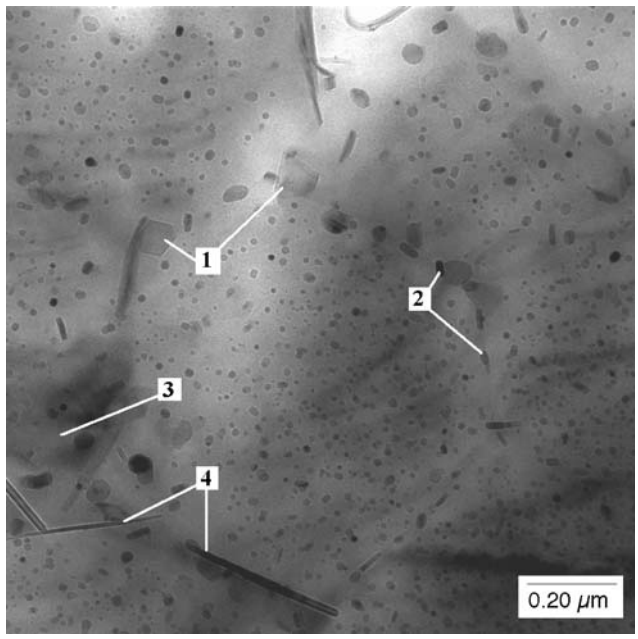

Fig. 7 TEM-micrograph

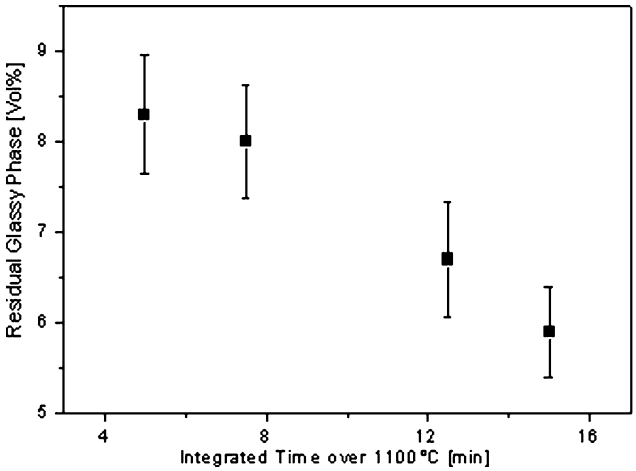

Fig. 8 Change of residual glassy phase with further heat treatment

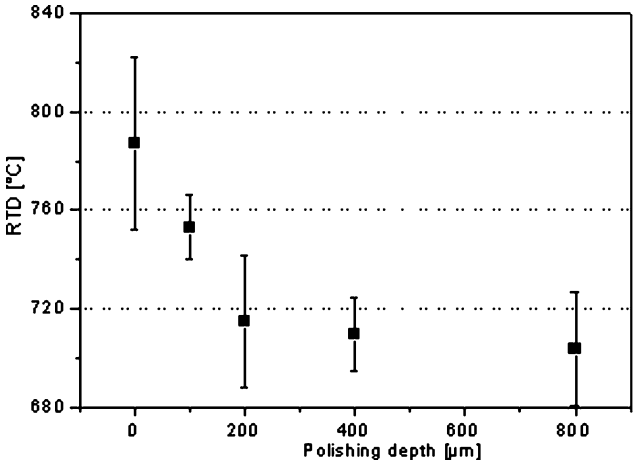

Fig. 10 Depth dependence of the RTD

residual glassy phase [Fig. 8] coupled with a slight crystal-growth (the well-known ''Ostwald-Miers ripening'') and a reduction of the lattice constants of the keatite s.s., as shown for the [001]-lattice constant [Fig. 9]. This decrease can be attributed to Si-incorporation in the keatite s.s., as confirmed by various authors [12–14].

Material properties of the glass–ceramic

Testing of carefully abraded and polished plates revealed that the RTD is depth-dependent. In Fig. 10 it is shown that the RTD decreases with increasing abrading-depth to a constant value in the bulk. This led to the assumption that gradients, presumably compressive surface stress-gradients, up to approximately 150 µm depth are responsible for an additional increase in breaking-strength.

In order to investigate these stresses, Vickers indentations at different loads (5 N, 10 N and 30 N) and XRD-stress-measurements were carried out on the material P_665, P_692, P_721, P_730, P_756, and P_777.

The load of the Vickers indentation is directly correlated with the crack length of the half-penny cracks, as explained previously. A SEM-image of a crack induced by Vickers indentation is shown in Fig. 11. The half-penny crack can be clearly seen and tests with loads equal to or higher than 3 N showed that no Palmquist cracks occur.

In Figs. 12, 13, 14 the correlation between RTD and crack length of different ceramized samples is shown. Samples with increased RTD show a decreased crack length. Also, with increasing load the obviously linear relationship between RTD and crack length weakens. With 30 N load, the reproducibility and the resolution of the RTD decrease significantly as a function of

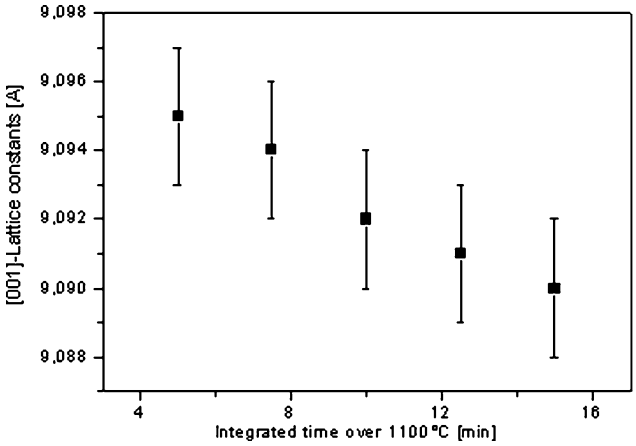

Fig. 9 Change of the [001]-lattice constants with further heat treatment

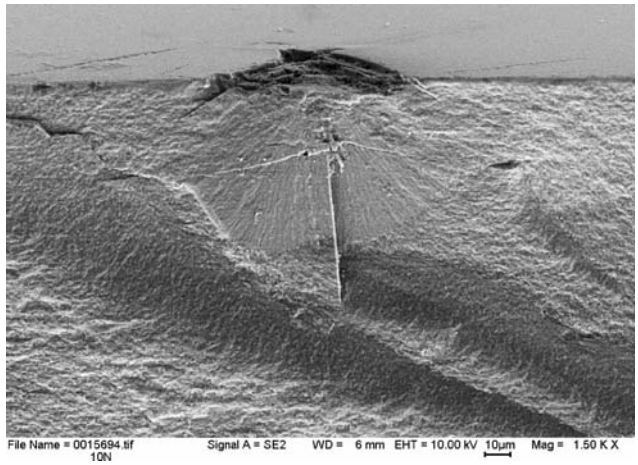

Fig. 11 SEM-image of a Vickers indentation at 10 N load, P_730

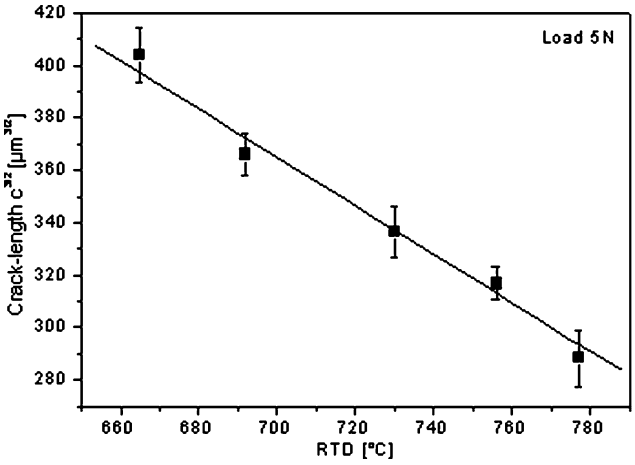

Fig. 12 Depth dependence of the RTD at 5 N load

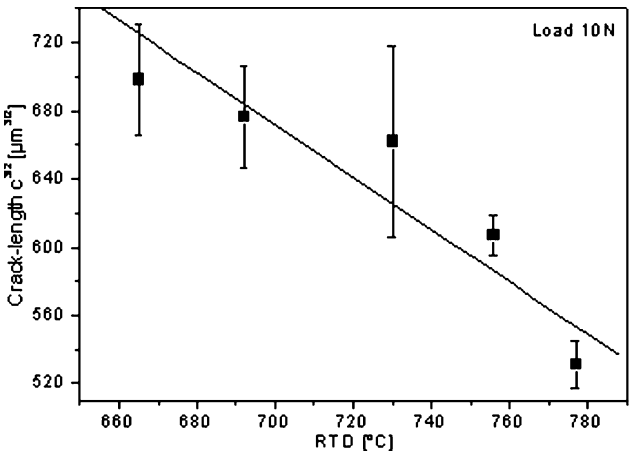

Fig. 13 Depth dependence of the RTD at 10 N load

depth (Fig. 14). This phenomenon can be attributed to a stress gradient, as explained in Eq. (6): the bulk-stresses σ_b start to influence the crack growth when higher loads and deeper cracks are applied.

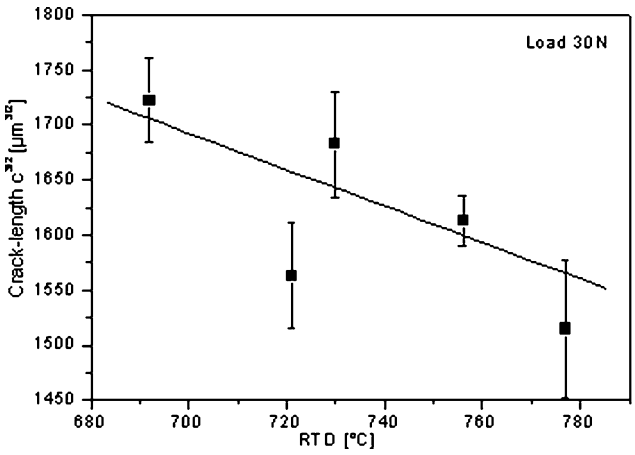

Fig. 14 Depth dependence of the RTD at 30 N load

The proportionality factor $F/c_i^{3/2}$, which is a direct measure for the crack length, was recorded over a depth of 200 µm. This was done by carefully polishing samples to the desired depth, before applying 30 Vickers indentations at a load of 5 N. Careful polishing ensured that the residual stresses were hardly affected by the process of material removing. The indentations were started at a depth of 8 µm. This was done to make sure that the indentations were not influenced by the layered structure mentioned earlier. The average $F/c_i^{3/2}$ of these 30 indentations for each depth is shown in Fig. 15. As can be seen, the average proportionality factor $F/c_i^{3/2}$ decreases with increasing depth, which corresponds to an increasing crack length. Therefore the stress distribution changes. Compressive stresses either decrease or change to tensile stresses in the bulk.

To investigate the nature of the stresses, X-ray stress measurements (RS-XRD) were carried out. As can be seen from Fig. 16, the stresses in the material are

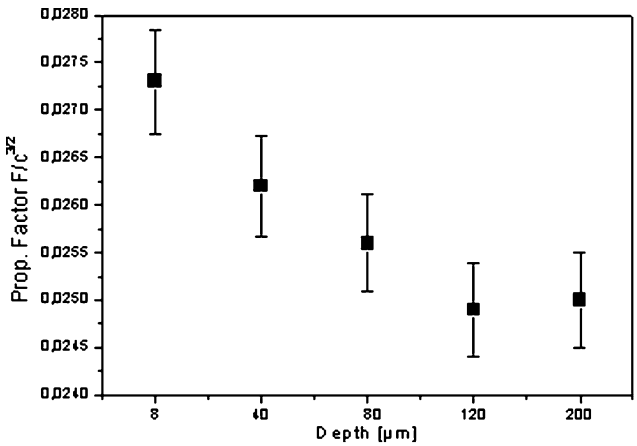

Fig. 15 Depth dependence of the crack length

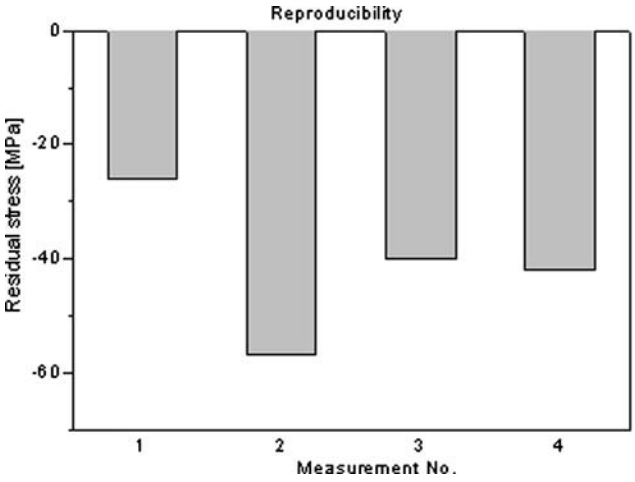

Fig. 16 Reproducibility of stress measurements (DS-XRS)

compressive. But with RS-XRD, in contrast to the Vickers-indentation method, it was not possible to resolve the stress differences of approximately 10 MPa, which cause the RTD variations. This was because of low sensitivity and reproducibility, which were due to different reasons: first, the compressive stresses are relatively small. Second and more important, only few, not-overlapping diffraction lines can be used for RS-XRD in the case of keatite s.s., the best located at 70° 2ϕ ($Cr_{K\alpha}$-radiation), which again is very low for RS-XRD-measurements. Because of this, only small peak shifts occur in this angle range.

The discussed results led to the assumption that stresses due to chemical gradients are responsible for the variation and depth dependence of the RTD. These chemical gradients occur over a thickness of about 150 μm if the material is ceramized as shown in Figs. 17 and 18 for Zn, K, and Si (measured by XRF). In the glassy material no chemical gradients were observed. Alkali elements, which are normally not incorporated in the keatite s.s. (that is all except Li), are depleted in the surface-near region, whereas Zn and presumably Li, which is in the same way incorporated in the crystal as Zn, are enriched (unfortunately Li is not measurable by XRF).

It is commonly known that Zn and Li decrease the CTE of LAS-glass–ceramics, whereas K increases it. The gradients therefore lead to a higher CTE in the interior of the material compared to the surface, and this results in surface-compressive stresses. The reason for these surface stresses are chemical gradients, which are supposedly caused by different transformation kinetics of the surface and the interior, resulting in diffusion of CTE-relevant elements. With appropriate ceramization, these gradients can be controlled to yield a RTD-range from approximately 660–780 °C.

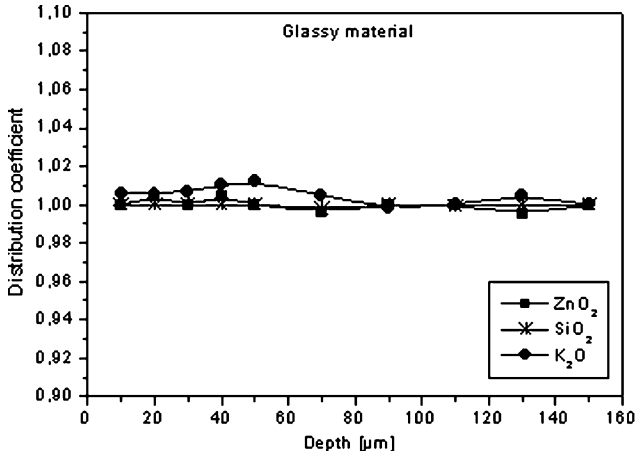

Fig. 17 Distribution coefficients over depth of various oxides in the glassy material

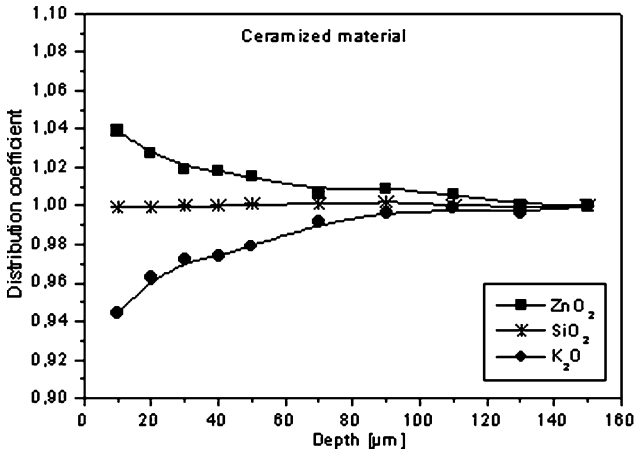

Fig. 18 Distribution coefficients over depth of various oxides in the ceramized material

Summary

The microstructure of a translucent keatite solid–solution glass–ceramic was investigated with SEM, AFM, XRF, XRD, and TEM. The glass–ceramic consists mainly of keatite s.s. with minor secondary phases such as zirconium titanate, gahnite and probably rutile. The remaining amount of glassy phase was analyzed to be less than 10 vol%. With further heat treatment a decrease in the amount of residual glassy phase was observed. This decrease is correlated with a decrease in the [001]-lattice constants of the keatite s.s., as has been reported by various authors. The keatite s.s. therefore incorporates Si with further heat treatment. This on the other hand leads to the observed decrease in glassy phase, which deplets in Si-concentration and enriches in the elements that are not compatible with the keatite s.s. structure.

It was also shown that compressive stresses can be induced into a fully transformed keatite s.s. glass–ceramic without aborting the transformation from high-quartz s.s. to keatite s.s.. These compressive stresses, caused by chemical gradients, lead to an increase of the RTD and can be controlled through the ceramization program. This is therefore useful to increase the strength and application range of glass–ceramics based on keatite s.s.

The fruitful discussions with G. Müller, Fraunhofer ISC Würzburg, and W. Pannhorst, Schott AG Mainz, are appreciated. The authors are grateful to J. Meinhardt, Fraunhofer ISC Würzburg, for the TEM-analysis. The theoretical stress considerations were done by courtesy of R. Dudek, Schott AG Mainz.

References

1. Scheidler H, Rodek E (1989) Ceram Bulletin 68(11): 1926
2. Allersma T (1980) Patent US 4,218, 512
3. Pannhorst W, Wichelhaus W (1983) Proc. 13th Int. Congr. On glass, 56K: 572
4. Zimmer J (1997) PhD Thesis, Uni Würzburg
5. Bach H (ed.) (1995) Low thermal expansion glass ceramics, Springer
6. Lawn BR, Fuller ER (1975) J Mater Sci 10: 2016
7. Evans AG, Proc. 11th Symp. on fracture Mechanics, ASTM 678, 83 (1978)
8. Anstis GR, et al. (1981) J Am Ceram Soc 64(9): 533
9. Munz D, Fett T (1989) Mechanisches Verhalten keramischer Werkstoffe, Springer
10. Lawn BR, Fuller ER (1984) J Mater Sci 19: 4061
11. Gruninger MF, et al. (1987) J Am Ceram Soc 70(5): 344
12. Hummel FA (1951) J Am Ceram Soc 34(8): 235
13. Fukasawa T, Iwatsuki M, Yamaguchi K (1973) Bunseki Kagaku 22(6): 745
14. Arnault L, Gerland M, Rivière A (2000) J Mater Sci 35: 2331